FRACTURE BEHAVIOUR OF ALKALI ACTIVATED CONCRETE MEASURED FROM THREE-POINT BENDING TEST WITH CHEVRON NOTCH

PETR MIARKA[*], LIXIA PAN[*†], VLASTIMIL BÍLEK[†], HECTOR CIFUENTÉS[**] AND STANISLAV SEITL[*††]

[*] Faculty of Civil Engineering, Brno University of Technology, (FCE-BUT)
Veveří 331/95, 600 02 Brno, Czech Republic
e-mail: petr.miarka@vut.cz, www.vutbr.cz

[*†] College of Mechanics and Materials, Hohai University, (HU)
Focheng West Road 8, 211100 Nanjing, China
plxxak@163.com, http://en.hhu.edu.cn

[†] Faculty of Civil Engineering, Technical University of Ostrava, (FCE-TUO)
L. Podéště 1875/17, 708 33 Ostrava, Czech Republic,
vlastimil.bilek@vsb.cz, www.vsb.cz,

[**] School of Engineering, University of Seville (US)
Camino Descubrimientos, S/N, Isla Cartuja, 41092 Sevilla, Spain
e-mail: bulte@us.es, www.etsi.us.es,

[††] Institute of Physics of Materials, Academy of Science of the Czech Republic (IPM)
Zizkova 22, 616 62 Brno, Czech Republic
e-mail: seitl@ipm.cz, www.ipm.cz

Key words: Three-point bending test, Chevron notch, Fracture Energy, Alkali Activated Concrete

Abstract: Specimens for the bending tests with the chevron notch are suitable for the evaluation of the fracture energy/toughness of civil engineering materials like concrete. The main advantage of this test set-up is that no sharp pre-crack has to be introduced, because a sharp crack is formed during loading at the beginning of the test. Furthermore, no crack length measurement is required, and a stable crack growth can be reached due to chevron geometry of the notch. In this contribution a difference of the ligament area of the specimens with the straight through notch and the chevron notch was investigated. The experimental campaign was performed on the alkali activated concrete three-point bending specimens tested with straight through notch and with the chevron notch. The specimens had the same ligament area in order to quantify the influence of the chevron notch boundary conditions on the value of the work of fracture and the fracture energy.

1 INTRODUCTION

Usually, the fracture properties of concrete are evaluated from a recommended geometry of three-point bending test with straight through notch in the mid span of the specimen [1]. This experimental set up, which provides stable and reliable results, is acknowledged among the researchers. The need of knowledge of the fracture behaviour of concrete had arisen in recent years with the development of increasingly powerful computers, which reduces the convergence time of the numerical calculations. This fact, allowed the use of non-linear material models of concrete in the design of important structures, more widely e.g. bridges, cooling towers, sea walls, nuclear vessels etc. However, this numerical model

usually uses numerous input parameters, which have to be calibrated before the beginning of the numerical analysis [2][3][4][5]. Nevertheless, the value of fracture energy is always the major input parameter as it is closely related to crack initiation, which also directly influences the durability within the structure lifetime.

On the contrary, there is no agreement among researchers on the definite geometry shape which could provide the independent value of the fracture energy G_f [6][7][8][9].

In this contribution the applied testing technique for evaluation of the fracture energy is the chevron-notched beam test (CNB). This experimental technique is a standardized method to evaluate fracture toughness of ceramics [10] and [11], also used for brittle metals like bearing steel [12] or aluminium alloys [13]. Experimental bending test set-ups with specimens possessing a chevron notch have been introduced and standardized since the 1960's [14][15]. The advantage of this test set-up is that no sharp pre-crack has to be introduced because a sharp crack is formed during loading at the beginning of the test [16]. Furthermore, no crack length measurement is required, and a stable crack growth can be reached due to the geometry of the notch [17][18][19].

In the load-displacement relations (See Fig. 1), the area enclosed by the response curve represents the work done by the external load to produce fracture of the specimen/beam. Suppose that the crack growth is stable, and the work done by external load is spent entirely in crack propagation. Based on the Griffith energy criterion [20], crack growth in an elastic body in the equilibrium state is a natural process of energy transfer between the strain energy of the body and the fracture energy required for creating a new crack surface, so that a state of minimum potential energy is achieved for the system at a given load level. In the present case, the work is consumed in breaking the unnotched part of the beam's cross-section – the ligament area in front of the notch.

According to the RILEM method [1] and Karihaloo [21][22], for three-point bending test (3PB) on notched specimens, the work of the external force (fracture value) W_F, is obtained from the complete load – displacement (P-d) diagram as follows:

$$W_F = \int P(d)dd \tag{1}$$

The value of the specific fracture energy G_F (energy needed to create a crack of unit area) can be expressed as:

$$G_F = \frac{W_F}{A_{lig}}, \tag{2}$$

where W_F is the work of fracture calculated from eq. 1 and A_{lig} is the ligament area.

Karihaloo in [21] and in [23] discusses various notch depth on the evaluation of the specific fracture energy G_F. The notch depth has direct influence on the ligament area A_{lig}, hence the knowledge of A_{lig} is crucial in fracture of the brittle materials.

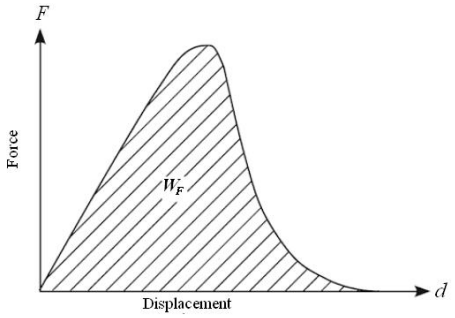

Figure 1: Determination of work of fracture W_F based on the RILEM method: notched beam under three-point bending and load deformation relations (adopted from [1]).

(a)

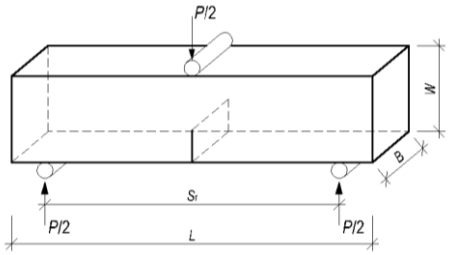

(b)

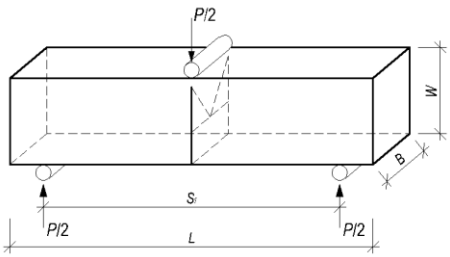

Figure 2: Sketches of 3PB specimen with straight through notch (a) and 3PB specimen with chevron notch (b).

Specimens with the same initiation length of the chevron notch has a smaller ligament area $A_{lig,chevron}$ compared to the standard specimens with the straight through notch A_{lig}, therefore more specific fracture energy is needed for the fracture process.

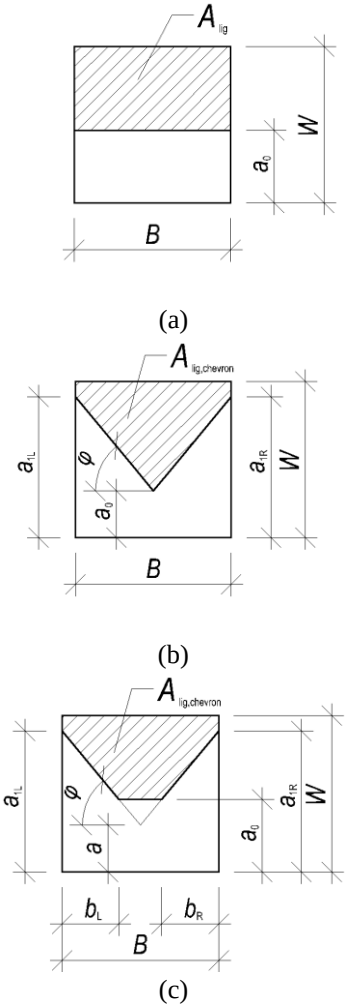

Figure 3: Comparison of ligament area of straight through notch (a), chevron notch with constant angle (b) and chevron notch with constant angle with blunt ending (c).

The examples of the various notch endings are shown in Fig. 3. The straight notch is sawed by on cut in the specimen i.e. notch length is a_0. The relative crack length is then expressed as a a_0/W or α_0, where W is the width of the specimen (See Fig. 3(a)). Whether in case of the chevron notches, there can be two types of notches sharp or blunt chevron notch. To produce such a notches two or more cuts are necessary. In case of sharp notch, the relative crack length is expressed by two parameters α_0 and α_1. The parameter α_0 express the position of the sharp end of the chevron notch, while the α_1 denotes the notch length at the edge of the specimen (See Fig. 2(b)).

In order to quantify difference of specimen's ligament area a constant value of a_0 (α_0 is then calculated as a a_0/W, where W represents the width of the specimen) with notch angle φ equal to 45° for the sharp chevron notch. This helps to identify the difference of the ligament area on the measured work of fracture W_f and fracture energy G_f. The definition of the cross-section with the straight through and sharp chevron notches shows Fig. 3.

The aim of this contribution is to quantify the influence of various notches on the value of fracture energy. For this purpose, an experimental campaign was prepared on specimens with various geometry notches, but with similar dimensions, i.e. thickness, width and span. Load-displacement (P-d) curves were measured and compared for specimens with the straight through notches and chevron notches. The numerical models with model of concrete material were prepared and compared.

2 NUMERICAL MODEL

In order to assess the relevance of the 3PB with a chevron notch, a numerical study of a 3PB with and without the chevron notch was performed using the finite element (FE) software ATENA-science [24][25]. For this, a three-dimensional (3D) was created with a dimension of B = 80 mm × W = 80 mm × S = 200 mm corresponding to the specimen's size in experimental tests. The beams had an initial notch length a of 24 mm corresponding to a relative crack length a/W = 0.3, an initial notch thickness t of 2 mm. The chevron notch had dimensions of a_0 = 0 mm and a_1 = 45 mm. This chevron notch ligament area has a same ligament area as a straight through notch of a/W = 0.3.

The numerical study was performed with a displacement-controlled loading applied at the top support of the studied geometry, while the bottom supports were considered as a rigid support. The total induced vertical displacement of top support was u_Y = -1 mm (u_X = 0 mm) over the pseudo time step (static analysis).

Adequate boundary conditions were added to prevent rigid body translations (See Figure 4).

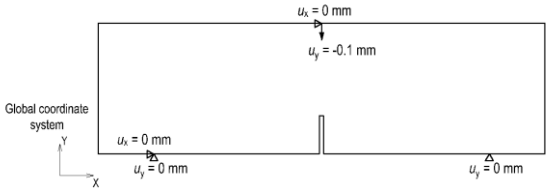

Figure 4: Boundary conditions used in the numerical simulation.

The numerical model was meshed with a 20-node linear hexahedral element referred as 3D beam element in ATENA's documentation. A meshed numerical model is shown in Figure 5(a) for straight through notch and in Figure 5(b).

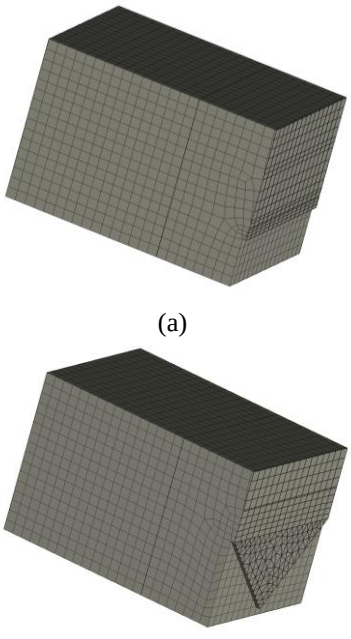

(a) (b)

Figure 5: Comparison of meshed numerical models straight through notch (a) and chevron notch (b).

A fine mesh (Figure 6) with a basic element size of 5 mm was studied with refinements around the notch tip of 2 mm. This model shows a mapped mesh pattern, which was crucial to get accurate numerical results. The mapped mesh was created by using sufficient partitioning and refinement of the geometry. The details of meshed ligament area are shown in Figure 6.

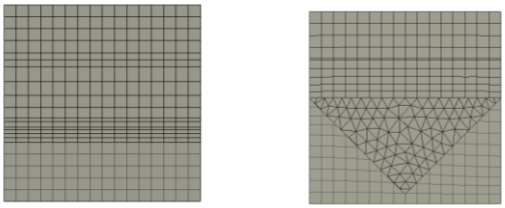

(a) (b)

Figure 6: Comparison of the detail of straight through notch (a) and chevron notch (b).

A 3DCementitious material model was used in numerical model, which is characterized as fracture-plastic model for concrete modelling. The input material parameters used in numerical model were Young's modulus E = 30 GPa, Poisson's ratio ν = 0.2. The compressive strength f_{cm} was set to 50 MPa, with crushing limit $f_{c0} = 0.4 \times f_{cm}$ = 20 MPa and the tensile strength f_{ct} = 5 MPa. The post-peak tensile softening branch uses Hoordijk's exponential function [26] with the fracture energy G_f = 150 N/m.

The generated load against the deflection of specimen at mid span the *P-d* diagrams are presented in Figure 9 and in Figure 10 to give a comparison with experimental *P-d* diagrams.

3 EXPERIMENAL PROCEDURE

In order to verify the numerical simulation an experimental program was done consigning of three specimens straight through notch and two specimens with chevron notch. The experimental results are presented in what follows.

3.1 Material

Alkali activated concrete (AAC) was designed based on formerly performed tests, see e.g. [27]. The mixture composition is shown in Table 1. The dry mass of activator was 8 % and the water to slag ratio was 0.45. Sodium water glass and potassium hydroxide

were combined to reduce efflorescence (see [28]) and an appropriate silicate modulus of activator (M_s = 0.67 or mass ratio (K_2O + Na_2O) / SiO_2 is 60/40). This composition of activator is convenient in terms of both setting and strengths. Naphthalene based plasticizer was also used for better workability of the mixture. The cone flow of the mixture was 600 mm.

Table 1. Composition of alkali activated concrete.

	GBFS	Na-WG M_s = 2.0	50 % solution of KOH	water	PSN-plasticizer	sand 0/4 mm	crushed aggregates 4/8 mm	crushed aggregates 8/16 mm
[kg/m^3]	450	45	34	159	10	855	385	400

Table 2. Mechanical properties of alkali activated concrete.

f_c – 24 h - cubes 150 mm	8.8 ± 0.3 MPa
f_c – 14 d - cubes 150 mm	53.4 ± 1.2 MPa
f_c – 28 d - cubes 150 mm	62.0 ± 1.5 MPa
f_c – 28 d - cylinders 150 × 300 mm	48.0 ± 3.4 MPa
f_{ct} – 28 d - cubes 150 mm	3.4 ± 0.2 MPa
E_{stat} – 28 d - cylinders 150 × 300 mm	26.3 ± 1.1 GPa
E_{dyn} – 28 d – cylinders 150 × 300 mm	29.6 ± 3.3 GPa

To test the mechanical properties, 150 mm cubes and 150 mm diameter and 300 mm height cylinders were prepared - see Table 2. All the specimens were carefully enveloped with PE-foil (to prevent moisture exchange with the environment) and stored outside the laboratory (temperature ≈ 5 - 25°C for 28 days).

From the point of view of mechanical properties, the AAC shows a low early strength, but over time the values of compressive strength increase and ultimately reach relatively high values. Compared to ordinary Portland cement-based concrete of similar strength, the AAC shows a significantly lower value of modulus of elasticity - see also [30].

3.2 Geometry and dimensions

The specimens for the experimental testing had dimensions of 80 mm × 80 mm × 220(200) mm (width W × thickness B × length L
(span S)). The notches have been prepared with diamond saw with a thickness of approx. 2 mm. The machine for tests has a maximum loading capacity 200 kN. The speed of the induced displacement of the upper support was equal to 0.025 mm/s. The experimental set up is shown in Figure 7.

In total five specimens were experimentally tested to evaluate the work of fracture W_f and fracture energy G_f and to quantify the influence of the different notch type. The specimens 1-3 had straight through notch, while the specimens 4 and 5 had chevron notch.

Figure 7: Actual experimental set-up.

The dimensions of notches prepared by diamond saw with thickness of 2 mm are presented in Table 3.

Table 3: Dimensions of ligament area.

Specimen	a [mm]	a_1 [mm]	b_1 [mm]	A_{lig} [m^2]
1	24.2	0	0	0.0045
2	23.4	0	0	0.0045
3	23.5	0	0	0.0045
4 - ChN	0	45.2	39.4	0.0047

5 - ChN	0	43.3	38.7	0.0047

These notches dimensions had been chosen to have same ligament area for both notch types, in order to normalize its influence on the fracture energy $G_{f.}$

The damaged specimen's ligament area is presented in Figure 8.

Figure 8: Damaged specimen with chevron notch.

4 RESULTS AND DISSCUSION

Firstly, the quantification of the measured value of work of fracture W_f and the fracture energy G_f is presented and then the comparison of the numerical and experimental *P-d* curves measured on 3PBT specimens with and without chevron notch made from the AAC material are presented in what follows.

4.1 Load-displacement curves

The experimental *P-d* diagrams for the straight through notch shows les stiff response (drop in post peak branch) than the chevron notch specimens. The numerically generated *P-d* curves shows major difference with experimental ones.

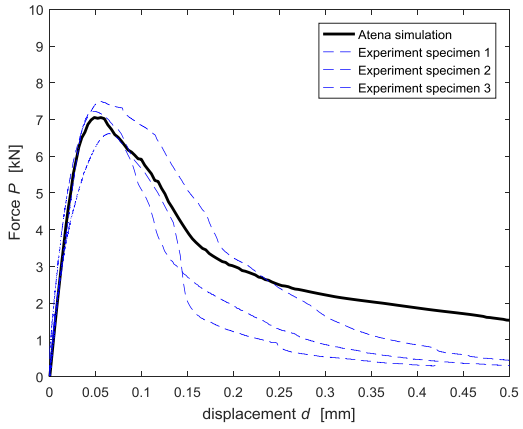

Figure 9: Comparison of experimental and numerical load displacement curves for blunt notch of relative crack length $a/W = 0.3$.

Nevertheless, the similar observation of higher stiffness for the specimen with chevron notch can be drawn. The comparison of numerically generated and experimentally measured *P-d* diagrams is shown in Figure 9 for straight through notch and in Figure 10 for chevron notch specimens.

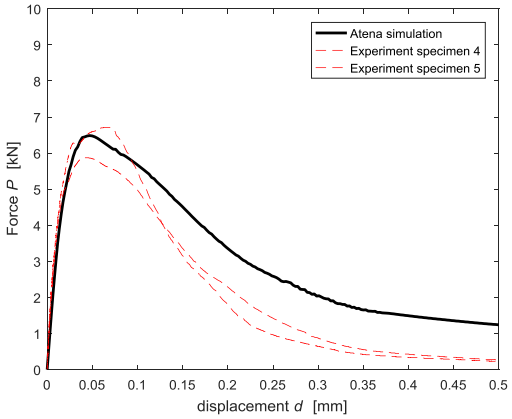

Figure 10: Comparison of experimental and numerical load displacement curves for chevron notch of relative crack length $a/W = 0.3$.

4.2 Work of Fracture and Fracture Energy

The work of fracture W_f was evaluated using Simpson's rule from experimentally measured *P-d* curves. From this a fracture energy Gf was calculated as a W_f/A_{lig} for each specimen. Overview of measured W_f and G_f is shown in Table 4, while the comparison of average W_f and G_f is shown in Table 5.

Table 4: Overview of measured work of fracture W_f and fracture energy G_f for various notch types.

Specimen	W_f [Nmm]	G_f [N/m]
1	0.935	208.714
2	1.171	261.150
3	1.099	245.397
4 - ChN	1.153	246.019
5 - ChN	1.261	266.024

Table 5: Comparison of average fracture energy on specimens with various notch types.

Notch type	Straight	Chevron
Fracture energy G_f [N/m]	238	256

From Table 5 a similar observation can be drawn as from *P-d* diagrams, that the chevron

notched specimens give a difference in measured G_f of 7.5 %. This effect should be taken into account in evaluation of fracture energy from specimens with chevron notches as the fracture energy is one of the main parameter inputs in the non-linear structural analysis. Similar trend could be seen in [30], where experimental results of fracture behavior of specimens with different cross sections are available. It was obtained more ductile behavior for specimens with trapezoidal sections (with increasing width) and for inverted T-sections and in [31], where the thickness effect on the fracture energy of cementitious materials based on a local fracture energy concept was shown/approved.

5 CONCLUSIONS

The influence of the various notch type for similar thickness on the value of the fracture energy was studied in both directions: numerically and experimentally. In total, two types of notch in span of three point bending 3PB test specimen had been investigated e.i straight through notch and chevron notch. From above presented results the following conclusions can be drawn.

The notch type directly influences an overall response of the 3PB specimen i.e. the specimen with chevron notch is stiffer than the specimen without the chevron notch. This has been verified by numerical model and experimental measurement. The notch directly influences the value of fracture energy. In was shown that the type of energy is influenced by difference limited to 8%.

To verify these drawn conclusions more into detail a new experimental measurement with various notch depths will be performed to give comprehensive results.

ACKNOWNLEDGEMENTS

This paper has been written with financial support from the Ministry of Education, Youth and Sports of the Czech Republic 8J18AT009 (Failure initiation and fracture of quasi-brittle building materials) and Brno University of Technology: projects FAST-J-19-5783 and FAST-S-18-5614 and from the support of the Czech Science Foundation: project GJ18-12289Y, as well as from the Spanish Ministry of Economy and Competitiveness under project BIA2016-75431-R.

REFERENCES

[1] RILEM TC-50 FMC 1985. *Recommendation. Determination of the fracture energy of mortar and concrete by means of three-point bend test on notched beams*. Materials & Structures. **18**:285–290.

[2] Lee, J., Fenves, L. G., 1998. *Plastic-Damage Model for Cyclic Loading of Concrete Structures Journal of Engineering Mechanics,* **124:***892-900.*

[3] Grassl, P., Xenos, D., Nyström, U., Rempling, R., Gylltoft, K., 2013. *CDPM2: A damage-plasticity approach to modelling the failure of concrete* International Journal of Solids and Structures, **50**:3805-3816.

[4] Hillerborg. A., 1985. *The theoretical basis of a method to determine the fracture energy GF of concrete.* Materials and Structures, **18:**291-296

[5] Bažant, Z. P., Oh, B. H., 1983. *Crack band theory for fracture of concrete.* Matériaux et construction, **16(3)**:155-177.

[6] Linsbauer, H., Tschegg, E., 1981. *Fracture energy determination of concrete with cube-shaped specimens.* Zement und Beton, **31**:38-40

[7] Cifuentes, H., Lozano, M., Holušová, T., Medina, F., Seitl, S., Fernandez-Canteli, A., 2017. *Modified disk-shaped compact tension test for measuring concrete fracture properties.* International Journal of Concrete Structures and Materials, **11(2)**:215-228.

[8] Cifuentes, H., Karihaloo, B.L., 2013. *Determination of size-independent specific fracture energy of normal- and high-strength self-compacting concrete from wedge splitting tests* Construction and Building Materials, **48**:548-553

[9] Malíková, L., Veselý, V., Seitl S., 2016. *Crack propagation direction in a mixed mode geometry estimated via multi-parameter fracture criteria* International Journal of Fatigue, **89**:99-107.

[10] *DIN EN 14425-3* 2010. *Advanced technical ceramics - Test methods for determination of fracture toughness of monolithic ceramics - Part 3: chevron notched beam (CNB) method.*

[11] ASTM C-1421-01b 2001. *Standard Test Methods for Determination of Fracture Toughness of Advanced Ceramics at Ambient Temperature.*

[12] Dlouhy I., Holzmann, M., Man J., Valka L., 1994. *The use of chevron notched specimen for fracture toughness determination of bearing steels*, Kovové Materiály -Metal Materials. **32(1)**:3–13.

[13] Calomino, A., Bubsey, R., Ghosn, L.J., 1994. *Compliance Measurements of Chevron Notched*

Four Point Bend Specimen. NASA Technical Memorandum 106538.

[14] Tatterall, H.G., Tappin, G., 1966. *The work of fracture and its measurement in metals, ceramics and other materials.* Journal of Materials Science. **1(3)**:296–301.

[15] Munz, D., Bubsey R.T. J.E. Srawley, J.E., 1980. *Compliance and stress intensity coefficients for short bar specimens with chevron notches.* International Journal of Fracture. **16(4)**:359–374.

[16] Munz, D., Shannon, J.L., Bubsey, R.T., 1980. *Fracture toughness calculation from maximum load in four point bend tests of chevron notch specimen*. International Journal of Fracture. **16**:137-141.

[17] Munz, D., Bubsey, R.T., Shannon, J.L., 1980. *Fracture toughness determination of A12O3 using four-point-bend specimens with straight-through and chevron notches.* Journal of American Ceramic Society. **63 (5–6)**:300–305.

[18] Seitl, S., Miarka, P., Sobek J., Klusák, J., 2017. *A numerical investigation of the stress intensity factor for a bent chevron notched specimen: Comparison of 2D and 3D solutions.* Procedia Structural Integrity, **5**:737–744.

[19] Šimonová, H., Daněk, P., Frantík, P., Keršner, Z., Veselý, V., 2017. *Tentative Characterization of Old structural concrete through mechanical fracture parameters.* Procedia Engineering **190**:414–418.

[20] Anderson, T.L. 2017. *Fracture mechanics: Fundamentals and applications.* CRC press.

[21] Karihaloo, B. L, 1995. *Fracture Mechanics and Structural Concrete.* Addison Wesley Longman, UK.

[22] Karihaloo, B.L., Nallathambi, P., 1990. *Effective crack model for the determination of fracture toughness (KIce) of concrete.* Engineering Fracture Mechanics. **35(4–5)**:637-645.

[23] Karihaloo, B.L., Abdalla H.M., Imjal, T., 2003. *A simple method for determining the true specific fracture energy of concrete. Magazine of Concrete Research*. **55(5)**:471-481.

[24] Červenka, V., Jendele, L., Červenka, J., 2010. *ATENA Program Documentation*, Cervenka Consulting, Prague.

[25] Červenka, V., Červenka, J., Pukl, R., 2002. ATENA / A tool for engineering analysis of fracture in concrete, Sadhana-Adacemy Proceedings in Engineering Sciences, **27**:485–492.

[26] Hordijk, D. A., 1991. *Local approach to fatigue of concrete*. Doctoral Thesis TU Delft,

[27] Bilek V., Opravil, T., Soukal, F., 2010. *Searching for practically applicable alkali-activated concretes*. 1st Int. Conf. on Advances in Chemically-Activated Materials 28-35.

[28] Szklorzová, H., Bílek, V., 2008. *Influence of alkali ions in the activator on the performance of alkali activated mortars*. Proc. of 3rd International Symposium Non-Traditional Cement and Concrete, 777 – 784.

[29] Sucharda, O., Bilek, V., Mateckova, P., Pazdera, L. 2018. *AAM for Structure Beams and Analysis of* Beam without Shear Reinforcement. Solid State Phenomena, **292**:3-8,

[30] Cifuentes, H., Medina, F., 2012. *Experimental fracture behavior of polypropylene fiber reinforced concrete, specimens with variable width*, Key Engineering Materials, **488-489**, 642-645

[31] Duan, K., Hu, X.-Z., Wittmann, F.H. 2003 *Thickness effect on fracture energy of cementitious materials*, Cement and Concrete Research, **33(4)**: 499-507.